Basin-scale spatio-temporal variability and control of phytoplankton photosynthesis in the Baltic Sea: the first multiwavelength Fast Repetition Rate fluorescence study operated on a ship-of-opportunity

Emilie Houliez[1*], Stefan Simis[1, 2], Susanna Nenonen[1], Pasi Ylöstalo[1], Jukka Seppälä[1]

[1] Finnish Environment Institute SYKE, Marine Research Center, Erik Palménin Aukio 1, 00560 Helsinki, Finland

[2] Plymouth Marine Laboratory, Prospect Place The Hoe, Plymouth, United Kingdom, PL1 3DH

* Corresponding author: emilie.houliez@outlook.fr

Abstract

This study presents the results of the first field application of a flow-through multi-wavelength Fast Repetition Rate fluorometer (FRRF) equipped with two excitation channels (458 and 593 nm). This device aims to improve the measurement of mixed cyanobacteria and algae community's photosynthetic parameters and was designed to be easily incorporated into existing ferrybox systems. We present a spatiotemporal analysis of the maximum photochemical efficiency (F_v/F_m) and functional absorption cross section (σ_{PSII}) recorded from April to August 2014 on a ship-of-opportunity commuting twice per week between Helsinki (Finland) and Travemünde (Germany). Temporal variations of F_v/F_m and σ_{PSII} differed between areas of the Baltic Sea. However, even though the Baltic Sea is characterized by several physico-chemical gradients, no gradient was observed in F_v/F_m and σ_{PSII} spatial distribution suggesting complex interactions between biotic and abiotic controls. σ_{PSII} was sensitive to phytoplankton seasonal succession and thus differed according to the wavelength used to excite photosystems II (PSII) pigments. This was particularly true in summer when high $\sigma_{PSII}(593)$ values were observed later and longer than high $\sigma_{PSII}(458)$ values, reflecting the role of cyanobacteria in photosynthetic light uptake measured at community scale. In contrast, F_v/F_m variations were similar after excitation at 458 nm or 593 nm suggesting that the adjustment of F_v/F_m in response to environmental factors was similar for the different groups (algae vs. cyanobacteria) present within the phytoplankton community.

Keywords: Fast repetition rate fluorometry, fluorescence, phytoplankton, Baltic Sea, ship-of-opportunity, ferrybox, primary production

1. Introduction

Phytoplankton primary production, the process by which microalgae and cyanobacteria produce organic matter using sunlight and atmospheric CO_2, forms the basis of the marine food web (Cloern, 1996; Falkowski and Raven, 2007) and defines the carrying capacity of aquatic ecosystems (Kromkamp et al., 2008). It is thus challenging to understand the functioning of a marine ecosystem and to sustainably manage its resources and health without a reliable estimate of phytoplankton primary production. The quality of this estimate in turn depends on our knowledge of the dynamics and processes controlling phytoplankton photosynthetic performances (Geider et al., 2001; Kromkamp et al., 2008).

Measurements of phytoplankton photosynthetic activity are not widely included in monitoring programs. Consequently, our estimates of phytoplankton primary production at the global scale and our knowledge of factors controlling phytoplankton photosynthesis are still crude (Falkowski and Raven, 2007; Lawrenz et al., 2013). Even in coastal areas with long running monitoring programs, such as the Baltic Sea, our understanding of the dynamics and controls of phytoplankton photosynthesis are limited to studies conducted occasionally or in spatially small areas (e.g. Müller and Wasmund, 2003; Raateoja et al., 2004a; Raateoja, 2004; Renk and Ochocki, 1998; Rydberg et al., 2006).

This scarcity of data can be explained by the prohibitive cost of operating studies from research vessels and from the methodological constraints associated with phytoplankton photosynthesis measurements. Phytoplankton photosynthesis has traditionally been measured as oxygen production (Gaarder and Gran, 1927; Montford, 1969) and carbon isotope uptake (Hama et al., 1983; Steemann Nielsen, 1952). These methods are sensitive but laborious (they require incubation) and are not easily automated (Marra, 2002). Carbon isotope uptake methods have also become increasingly difficult to apply due to stringent health, safety and environmental regulations (Robinson et al., 2014).

In the last decades, inducible fluorescence-based methods have been developed to measure phytoplankton photosynthetic parameters free from the constraints associated with the traditional methods (Suggett et al., 2010). Their use to conduct studies at large spatio-temporal scale and their incorporation into monitoring operations are, however, still limited. This slow adoption has been because commercially available instruments were not easily automated and incorporated into operational monitoring platforms. Additionally, the wavelength of light used to excite fluorescence could be non-optimal for phytoplankton communities with an important cyanobacterial component (Kromkamp and Forster, 2003; Raateoja et al., 2004b; Simis et al., 2012). Fast Repetition Rate fluorometers (FRRF) were initially equipped with a blue excitation light to approximate the spectral light quality in clear oceanic waters. Blue light, however, preferentially excites the photosystem II (PSII) antenna of algae containing chlorophylls *a/b/c* and photosynthetic carotenoids but greatly under-samples species with a low PSII cross section in the 400 - 500 nm region, relying instead on phycobilisomes rich in phycocyanin or long-wavelength variants of phycoerythrin, such as cyanobacteria and rhodophytes (Kromkamp and Forster, 2003, Raateoja et al., 2004b; Simis et al., 2012; Suggett et al., 2009). This makes the blue excitation light inappropriate in systems where cyanobacteria form an important component of the phytoplankton community such as in

72 the Baltic Sea and eutrophic freshwater environments (Raateoja et al., 2004b). Moreover, some

73 photosynthetic parameters, such as the functional absorption cross-section of photosystems II (σ_{PSII}), are

74 strongly species and wavelength-dependent. Consequently, relative changes in these parameters,

75 measured *in situ* on naturally mixed communities using just one excitation wavelength, can be properly

76 interpreted as temporal or spatial variations only if changes in the relative concentration of different

77 pigment types can be ruled out (Schreiber et al., 2012; Suggett et al., 2009).

78 There thus exists a need for variable fluorometers equipped with multiple light excitation

79 wavelengths to optimize the measurement of algae and cyanobacteria contributions in the fluorescence

80 signal measured at community scale (Simis et al., 2012). In recent years, commercial FRRF have been

81 brought to the market with two or three excitation wavebands to meet this need. One of these instruments,

82 the FFL-40 (Photon System Instruments, Czech Republic) was specifically designed to excite the pigment

83 groups present in mixed cyanobacteria and algae communities encountered in freshwater and coastal seas

84 and to be easily maintained while incorporated into ferrybox systems.

85 In this paper, we present the results of the first study testing this device in the acquisition of

86 phytoplankton photosynthetic parameters at basin scale with high spatial and temporal resolution from a

87 ship-of-opportunity in a marine system (the Baltic Sea) where mixed cyanobacteria and algae

88 communities occur naturally (Bianchi et al., 2000). This study is intended to provide a first proof-of-

89 concept of the FFL-40 in an autonomous flow-through setting operated during phytoplankton blooms and

90 the intermediate periods with low phytoplankton biomass. The primary objective of this work was to

91 characterize the spatio-temporal dynamics, along the dominant physicochemical and optical gradients in

92 the Baltic Sea, of two phytoplankton photosynthetic parameters describing the physiological state of

93 photosystems II (PSII): the maximum photochemical efficiency (F_v/F_m) and the functional absorption

94 cross section (σ_{PSII}). The second objective was to compare the photosynthetic parameters measured at

95 community scale using the two different excitation wavelengths of the FFL-40. Finally, this works aimed

96 to relate, to the extent possible, observed variability in photosynthetic parameters measured at both

97 wavelengths to environmental conditions observed from the ferrybox platform. Because the 458 nm

98 (blue) excitation light of the FFL-40 should be more efficient to excite the antenna pigments of algae

99 while the 593 nm (amber) light excitation corresponds better to the absorption peaks of antenna pigments

100 of cyanobacteria, different dynamics in F_v/F_m and σ_{PSII} measured at community scale using these both

101 wavelengths were expected. Further, because the Baltic Sea is characterized by several physicochemical

102 (temperature, salinity) and optical gradients, spatio-temporal variability in F_v/F_m and σ_{PSII} were expected

103 along these gradients. Finally, different spatio-temporal dynamics of F_v/F_m and σ_{PSII} between the

104 Helsinki-Travemünde (southward) and Travemünde-Helsinki (northward) transects were expected due to

105 sampling at different times during the day while F_v/F_m and σ_{PSII} are expected to exhibit a diel cycle.

106 F_v/F_m and σ_{PSII} are considered here because they are essential parameters to study phytoplankton

107 photosynthesis in nature (Suggett et al., 2009). F_v/F_m corresponds to the number of electrons produced as

108 the result of the absorption of a photon by a single separation event in photosystems II (PSII) (Kromkamp

109 and Forster, 2003). σ_{PSII}, also called PSII effective absorption, is a measure of the photochemical target

110 area size of PSII and corresponds to the product of absorption by the suite of PSII antenna pigments (*i.e.*

111 optical absorption cross section) and the probability that an exciton within the antenna will cause a

112 photochemical reaction (Mauzerall and Greenbaum, 1989; Moore et al., 2006; Suggett et al., 2009).

113 Under actinic light, F_v/F_m and σ_{PSII} both reflect how the absorbed light energy is used by PSII and both

114 parameters are strongly influenced by environmental conditions and phytoplankton community structure

115 (Suggett et al., 2009). Studying the response of these parameters to environmental conditions and

116 phytoplankton dynamics is thus fundamental to understand phytoplankton photosynthesis. Additionally,

117 they are needed to calculate electron transport rates (Silsbe et al., 2015; Suggett et al., 2004) and

118 subsequently feed into models of primary production.

119

120 **2. Materials and methods**

121 *2.1. Study area*

122

123   The Baltic Sea is a semi-enclosed non-tidal shelf sea surrounded by nine countries. It is the largest

124 body of brackish water in the world and is characterized by relatively stable gradients of salinity, coloured

125 dissolved organic matter (CDOM) and nutrient availability (Olli et al., 2011; Tamminen and Andersen,

126 2007). Narrow shallow straits in the western part offer the only limited water exchange with the North

127 Sea. The residence time of water in the Baltic Sea is estimated at 30 years (HELCOM, 2003). This limited

128 exchange rate combined with a high river discharge from a wide catchment area (approximately 1.7

129 million km²) results in high concentrations of nutrients, organic matter and pollutants in Baltic Sea

130 waters. Consequently, the Baltic Sea is severely affected by eutrophication and is considered as one of the

131 most polluted seas in the world (Lehtonen and Schiedek, 2006). Phytoplankton blooms in the Baltic Sea

132 include a high biomass spring bloom (between March and May) consisting mainly of diatoms and

133 dinoflagellates and a summer bloom (between June and August) dominated by filamentous cyanobacteria.

134 A late autumn bloom of varying composition is also occasionally observed. In the Baltic Sea,

135 cyanobacteria populations are composed of small-sized picocyanobacteria (mainly *Synechococcus sp.*)

136 and larger colony-forming filamentous N_2-fixing cyanobacteria dominated by *Nodularia spumigena*,

137 *Aphanizomenon flos-aquae* and *Dolichospermum sp.* (Hällfors et al., 2013; Stal et al., 2003).

138

139 *2.2. Sampling methodology*

140

141   Field measurements were carried out between April and August 2014 at high spatio-temporal

142 resolution from a ship-of-opportunity: "MS Finnmaid" commuting twice a week between Helsinki

143 (Finland) and Travemünde (Germany). The ship route nominally took 28 hours and covered the Western

144 Gulf of Finland, Northern Baltic Proper, Gotland Sea, Bornholm Basin, Arkona Sea and Mecklenburg

145 Bight *i.e.* 1132 km crossing several ecological areas of the Baltic Sea (Fig. 1). Water was pumped

146 continuously from 4 m-depth through the ferrybox measuring system and at specific locations, water

147 samples were collected for laboratory analyses (see further below). While the location of sampling

148 stations was somewhat variable between the different devices used, the ship route can be divided into 17

149 sampling zones as depicted in Fig. 1. The pumping system was switched to a washing cycle with diluted
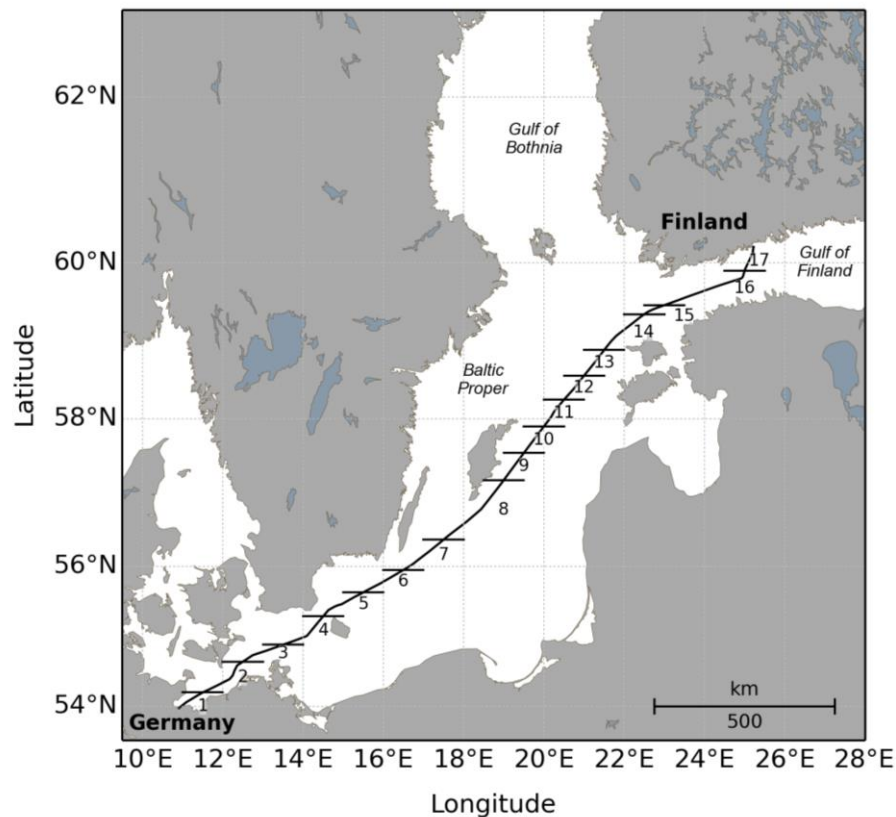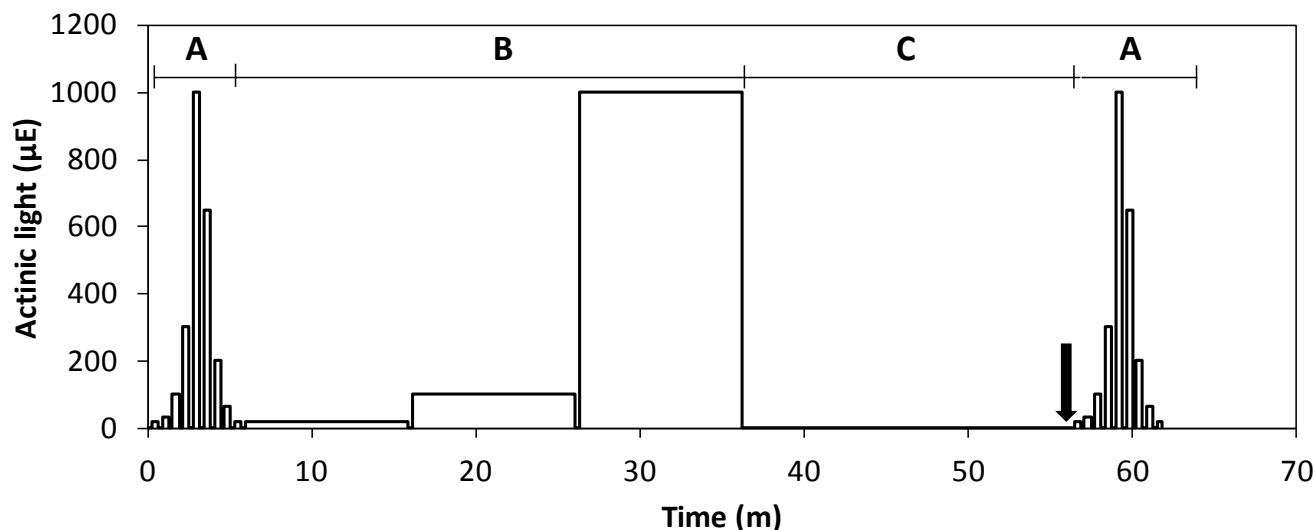
150 TRITON-X at each harbour.

151

152
153 **Fig 1.** Map of the Baltic Sea representing the ship route and sampling zones. Sampling zones correspond
154 to areas where the data set was complete (i.e. fast repetition rate measurements + physico-chemical
155 parameters measured from the ferrybox + physico-chemical parameters obtained from water samples) for
156 each sampling date

157

158 *2.3. Fast Repetition Rate fluorescence (FRRf)*

159

160 An FRRf measurement sequence (Fig. 2) was repeated every 68 minutes using the FFL-40 (Photon

161 System Instrument, Czech Republic). This flow-through FRR fluorometer is equipped with two banks of

162 light-emitting diodes (LED) providing flash excitation energy centered at 458 nm (blue) and 593 nm

163 (amber) and a 10 nm emission band pass filter around 690 nm coupled with a photodiode detector. A third

164 LED bank can provide actinic light from blue and amber LEDs. Excitation and detection wavelengths of

165 the FFL-40 were selected to optimize the measurements of the photophysiological parameters of naturally

166 mixed cyanobacteria and algae communities (Simis et al., 2012). However, it should be noted that

167 challenges in instrument design are much greater when combining longer wavelength (593 nm) excitation

168 with detection around 690 nm, compared to existing experience with blue excitation light. Isolating the

169 rise in fluorescence during a single turnover (ST) induction curve from cross-talked between light source

170 and detector requires careful and regular calibration of all optics in the system; a calibration that was

171 repeated weekly during this field study. Nevertheless, noise in data caused by variable cross-talk due to

172 light scattered by particles will always lead to reduced sensitivity in variable fluorescence at longer

173 excitation wavebands. The instrument is equipped with a measurement chamber exposed to excitation

174 flashlets and actinic light and a secondary chamber only exposed to actinic light. The secondary chamber

175 is kept at temperature by sea water flowing through an outer jacket of the chamber. The sample is

176 frequently redistributed between the chambers (between light steps and at one minute intervals during

177 dark acclimation) to prevent cells from settling and to maintain seawater temperature in the sample.

178

179
180 **Fig 2.** Measurement sequence. The actinic light intensity used during the different steps is represented. A:
181 Rapid light curves with five 10s increasing light steps and four 10s decreasing light steps. B: three 10min
182 increasing light steps. C: 20min dark acclimation. The black arrow represents the period when the
183 maximum photochemical efficiency (F_v/F_m) and functional absorption cross-section of photosystems II
184 (σ_{PSII}) were measured at 458 nm and 593 nm

185

186 Prior to each measurement sequence, detector gain and blue and amber flashlets intensity were

187 automatically adjusted to obtain optimal saturation. The intensity limits for blue and amber flashlets were

188 respectively 0 - 96,000 and 0 - 65,000 µmol photons m^{-2} s^{-1}. Actinic light was modulated between 0 and

189 1,000 µmol photons m^{-2} s^{-1} from blue and amber LEDs combined. The measurement sequence included

190 light response curves and measurements of fluorescence parameters before and after a period of dark

191 acclimation (Fig. 2). During this first deployment spanning the whole growth season, the protocol for

192 light response curves measurements was still being improved to obtain sufficient sensitivity during the

193 steps with the highest actinic light intensity. Therefore, only the fluorescence parameters measured at the

194 end of the 20 min dark acclimation are used in the present analysis. The FFL-40 was set to deliver ST

195 saturation of photosystems II (PSII) using a saturating sequence of 100 flashlets of 1 µs applied at 1 µs

196 interval. ST measurements with 458 and 593 nm excitation wavelengths were alternated at 1 s intervals.

197 After the 20 min dark acclimation, 74 fluorescence transient curves generated by the saturating sequence

198 were obtained for each excitation channel. These were each fitted to the Kolber-Prasil-Falkowski model

199 (KPF, Kolber et al., 1998) to extract the initial (F_0) and maximal (F_m) fluorescence levels, the

200 connectivity parameter (p) as well as the functional absorption cross-section of photosystems II (σ_{PSII}, in

201 $Å^2$ $quantum^{-1}$) and results were then averaged. The maximum photochemical efficiency was then

202 calculated for each channel as $F_v/F_m = (F_m-F_0)/F_m$. Analysis of filtrate (passed through Whatman GF/F

203 filters) from discrete samples collected along track (see below) and measured in the FRRF at the end of

the season indicated that background fluorescence (Cullen and Davis, 2003) was a minor source of error in F_v/F_m determination. The average percentage error equaled $10.7 \pm 6.1\%$ (n=133) for $F_v/F_m(458)$ and $1.3 \pm 1.1\%$ (n=48) for $F_v/F_m(593)$.

2.4. Physico-chemical parameters and phytoplankton dynamics

The FFL-40 was connected in a parallel water flow with the standard set of Alg@line ferrybox monitoring sensors which includes temperature, salinity, turbidity, and fluorescence of CDOM, chlorophyll *a* (chl *a*) and phycocyanin. All measurements were geolocated and time-stamped using GPS and ferrybox measurements were stored at 20 s-intervals, corresponding to a spatial resolution of approximately 200 m (for details on Alg@line ferrybox measurements see Leppänen et al., 1994; Rantajärvi et al., 2003; Ruokanen et al., 2003).

Temperature and salinity were measured with a SBE 45 MicroTSG thermosalinograph. Turbidity and chl *a* fluorescence were recorded with the WetLabs ECO FLNTU fluorometer. This device determines the turbidity based on light scattering at 700 nm while the chl *a* fluorescence is measured with an excitation waveband centered at 470 nm and an emission band centered at 695 nm. Phycocyanin fluorescence was recorded in relative units with a TriOS microFlu-blue fluorometer with an excitation waveband centered at 620 nm and emission at 655 nm. The combined use of fluorometers to measure chl *a*, phycocyanin as well as turbidity is suitable to follow phytoplankton groups dynamics in the Baltic Sea (Groetsch et al., 2014; Seppälä et al., 2007). CDOM fluorescence was measured with a TriOS microFlu-CDOM fluorometer with excitation at 370 nm and emission at 460 nm. The phycocyanin and CDOM fluorometers were installed on the ship from May 2014 onwards whereas the other parameters were measured throughout the studied period.

Downwelling irradiance above the water surface ($E_d(PAR)$) was measured every 15 s with a RAMSES ACC-VIS spectroradiometer (TriOS GmbH) that was part of the independently operating Rflex system to measure remote-sensing reflectance installed on the roof of the navigation bridge (Simis and Olsson, 2013). All $E_d(PAR)$ data presented in this publication are instant $E_d(PAR)$ measured at the same sampling stations as FFL-40 measurements.

Water samples were collected normally once a week at fixed stations on the return route of the ship (Travemünde to Helsinki) using an automatic refrigerated sequence sampler (Isco 3700 R). These samples were analyzed for nutrient concentrations ($NO_2^- + NO_3^-$, $Si(OH)_4$, PO_4^{3-}), chl *a* concentration and background FRR fluorescence. Nutrient concentrations were determined according to certified protocols for national monitoring contributions to the Helsinki Commission (HELCOM) and were based on colorimetric detection using a Lachat Quikchem FIA +8000 series analyzer. Nutrient Si:N:P ratios were compared to Redfield (1934) and Brzezinski (1985) ratios to characterize which nutrient was potentially limiting. Chl *a* concentrations were determined by concentrating known volumes of water samples onto Whatman GF/F glass-fibre filters. Pigment was extracted for 24h at room temperature (20-23°C) in 96% ethanol. Chl *a* concentrations in the extracts were quantified using a spectrofluorometer calibrated against

242   known concentrations of commercially purified chl *a* (Sigma) using excitation at 430 nm and emission at

243   672 nm with a slit width of 5 nm.

244

245   2.5. *Data analyses*

246

247   The significance of the relative contributions of transect sailing direction (i.e. southward or

248   northward), sampling zone and sampling date to the total variability of each physico-chemical and

249   photosynthetic parameter was evaluated using a mixed-effects nested ANOVA model. In this model, the

250   main factor (transect direction) was fixed and the nested factors (sampling areas within each transect and

251   sampling dates within each sampling area) were randomized. These analyses were performed using the

252   least squares method (method of moments) with JMP 12 software (SAS) following the instructions of Sall

253   et al. (2007).

254   To evaluate the spatial differences in physico-chemical parameters and phytoplankton composition

255   along the transect and identify areas with similar properties, a cluster analysis was performed using

256   PRIMER 6 (Clarke and Warwick, 2001). The variables incorporated were: sea temperature, salinity,

257   turbidity, CDOM fluorescence, E_d(PAR), nutrient concentrations, chl *a* and phycocyanin fluorescence.

258   For each sampling station, data were standardized, log transformed ($\log_{10}(x+1)$) and averaged over the

259   whole sampling period to limit temporal effects. The cluster was then built using the hierarchical

260   complete linkage method based on the similarity matrix obtained using the Euclidean distance. The

261   significance of differences between the groups identified by the cluster was verified with an analysis of

262   similarity (one-way ANOSIM test).

263   Relationships between photosynthetic parameters, environmental parameters and fluorescence

264   measurements of phytoplankton pigments were quantified using stepwise multiple linear regression

265   analyses with a forward procedure of selection using Statistica 6. The explanatory variables tested were:

266   sea temperature, salinity, turbidity, CDOM fluorescence, E_d(PAR), nutrient concentrations and

267   phycocyanin fluorescence. Chl *a* fluorescence was not included in this analysis because photosynthetic

268   parameters were extracted from FRRF measurements which also measure fluorescence from chl *a*. Our

269   hypothesis that sea areas with different physicochemical properties can reveal different factors

270   influencing on photosynthetic parameters was evaluated by applying stepwise multiple linear regression

271   analyses on data sets separated according to the areas identified by the cluster analysis. Before performing

272   these analyses, pre-analyses of correlations between the different environmental parameters tested have

273   been made using a matrix of Person's correlations. If several environmental variables were strongly inter-

274   correlated ($r > 0.8$), only one of these variables has been included in the stepwise multiple linear

275   regression analyses. For each area defined by the cluster analysis, a first stepwise multiple linear

276   regression analysis was realized using the reduced data set of sampling points where nutrient

277   concentrations were available. In the case where nutrient concentrations were not selected in the final

278   model of this first analysis, a second analysis using all available data and only testing the effects of sea

279 temperature, salinity, turbidity, CDOM, E_d(PAR) and phycocyanin fluorescence was performed. The

280 significance of each model was tested with F tests.

281   Significant differences between photosynthetic parameters measured at 458 and 593 nm were tested

282 with a paired t-test using Statistica 6 (Scherrer, 2007) and statistical relationships between these

283 photosynthetic parameters were evaluated with the Pearson product moment correlation using SigmaPlot

284 12.0.

285

286 **3. Results**

287 *3.1. Physico-chemical parameters*

288

289   Sea temperature, salinity, turbidity, CDOM and E_d(PAR) were not statistically different between the

290 southward (Helsinki-Travemünde) and northward (Travemünde-Helsinki) transects (ANOVA, P>0.05).

291 Sea temperature (Fig. 3A) varied significantly in space (i.e. between sampling areas, ANOVA, P<0.001)

292 and time (i.e. between each sampling date, ANOVA, P<0.001). Sea temperature was low in April (3.0°C)

293 and high in August (23.0°C). Sea temperature rise following the seasonal pattern was first visible in the

294 southern parts. Then the same temperature spread progressively to the northern areas and northern parts

295 reached the same temperature as southern parts in a few days. Salinity (Fig. 3B) ranged from 4.1 to 15.4

296 PSU. No significant temporal variation of salinity was observed (ANOVA, P>0.05). Spatially, there was

297 a significant decreasing gradient of salinity from the south to the north (ANOVA, P<0.001).

298      $NO_2^-+NO_3^-$ (Fig. 3C) and PO_4^{3-} (Fig. 3D) varied significantly in time (ANOVA, P<0.001) but not

299 spatially (ANOVA, P>0.05). $NO_2^-+NO_3^-$ ranged from 5.3 μM to concentrations close to the detection

300 limit (0.05 μM). The highest nutrient concentrations were observed at the beginning of the studied period

301 (April). $NO_2^-+NO_3^-$ concentrations subsequently decreased during the spring bloom to reach values close

302 to the minimum detection limit in May. The concentration of $NO_2^-+NO_3^-$ stayed low until August. PO_4^{3-}

303 concentration ranged from 0.7μM to concentrations close to the detection limit (0.1 μM) with highest

304 concentrations observed in April. PO_4^{3-} concentrations subsequently decreased until May-June and stayed

305 low until August. $Si(OH)_4$ concentration (Fig. 3E) ranged from 1.9 to 18.0 μM. $Si(OH)_4$ concentration

306 showed significant temporal variation (ANOVA, P<0.001) and the pattern of variation was different

307 between the different parts of the Baltic Sea (ANOVA, P=0.007). In the southern part of the transect

308 (from 54.2 to 55.5°N), $Si(OH)_4$ concentration was low in April and increased gradually until August. By

309 contrast, from 55.5 to 60.0 °N, $Si(OH)_4$ concentration was high in April and decreased until August. The

310 nutrient ratios Si:N and N:P were respectively well above and below the theoretical 16:16 and 16:1

311 proportions, nitrogen was consequently the most likely limiting nutrient.

312   Turbidity (Fig. 3F) varied significantly in space (ANOVA, P<0.001) and time (ANOVA, P<0.001).

313 Turbidity ranged between 0.70 and 4.07 NTU. Turbidity was relatively low and constant (<1.50 NTU)

314 except during July when a high turbidity (with a peak at 4.07 NTU) was recorded in the northern part of

315 the transect (between 57.9 and 60.0°N).

316   No significant temporal variation of CDOM fluorescence (Fig. 3G) was observed (ANOVA,

317   P>0.05) whereas spatially, a significantly increasing gradient of CDOM fluorescence was observed from
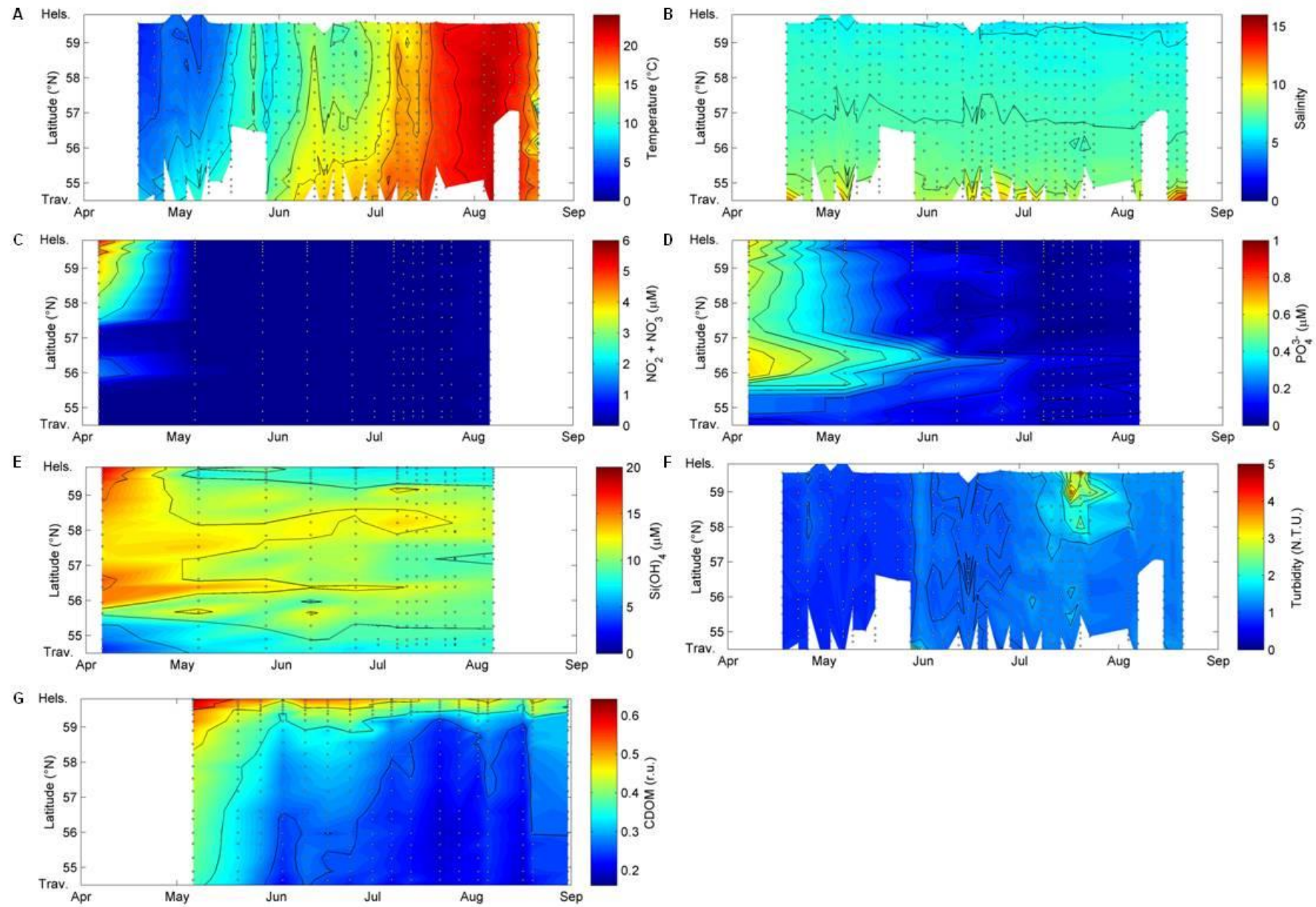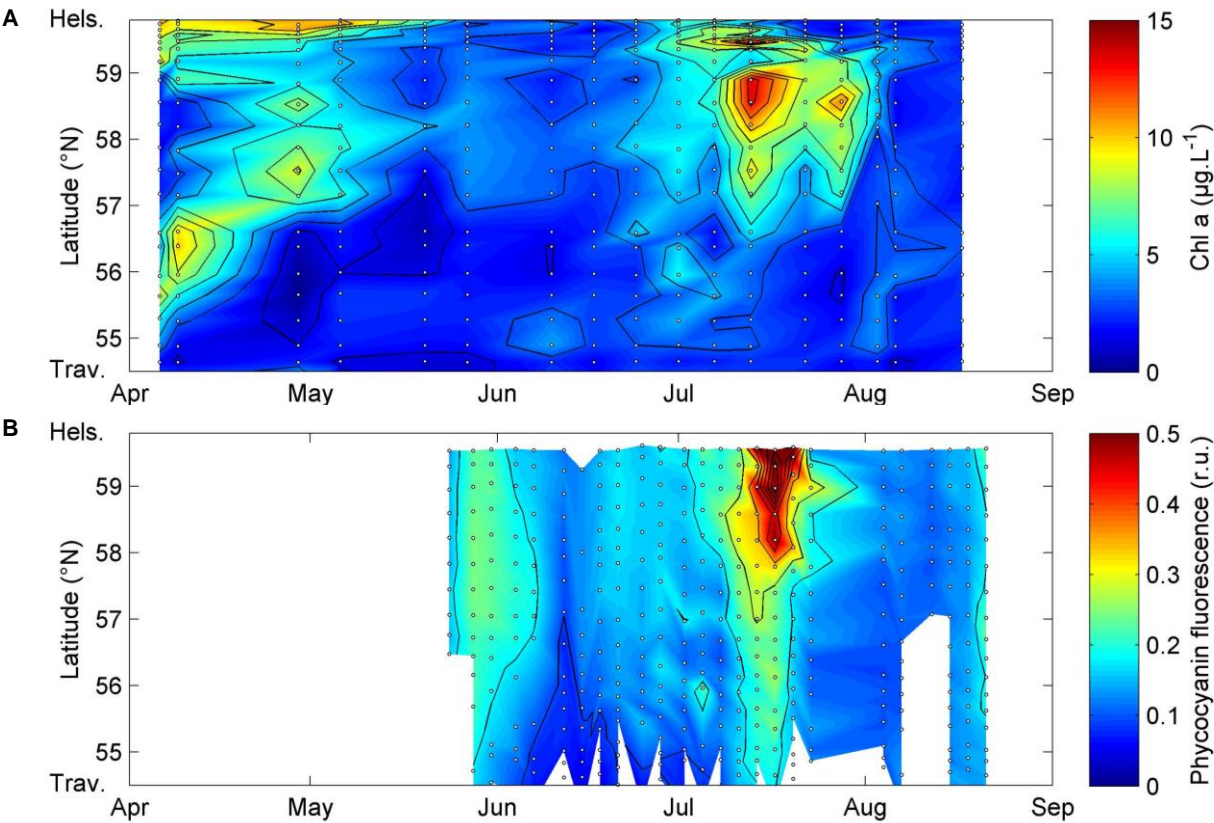
318   the south to the north (ANOVA, P<0.001).

Fig 3. Spatio-temporal variation of A) temperature (°C), B) salinity (PSU), C) $NO_2^-+NO_3^-$ concentration (µM), D) PO_4^{3-} concentration (µM), E) $Si(OH)_4$ concentration (µM), F) turbidity (NTU) and G) coloured dissolved organic matter (CDOM)

319   Spatial patterns in E_d(PAR) measurements clearly revealed the sampling constraints associated with

320   the use of a ship-of-opportunity for photophysiological measurements. Due to the regular sailing schedule

321   of the ship, areas located between 57.0 and 59.5°N were always sampled at night while others areas were

322   sampled in daytime. Temporal variations of E_d(PAR), in the areas sampled in the daytime, followed the

323   typical temporal variations of temperate northern regions with an increasing E_d(PAR) from April to

324   August.

325

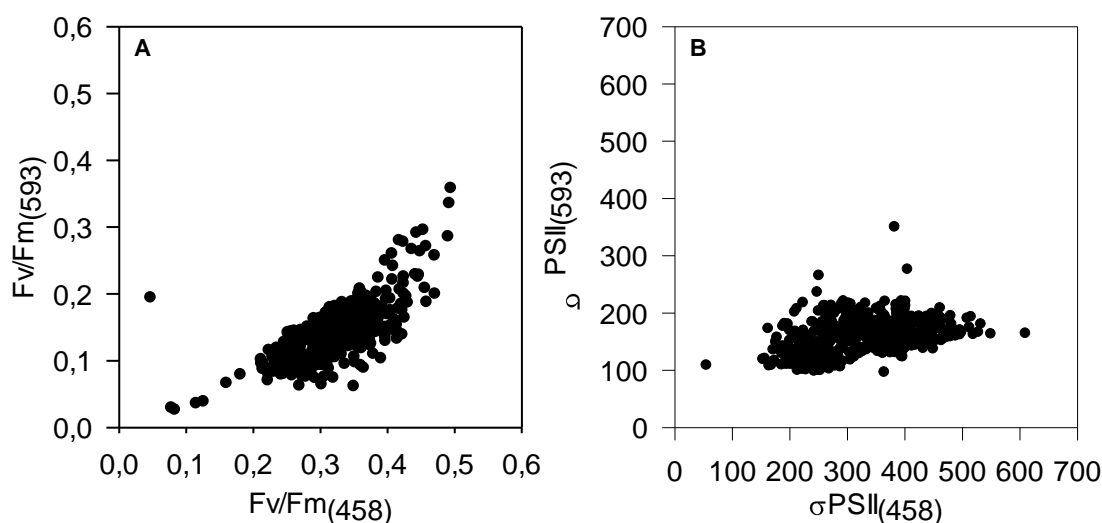326   *3.2. Extracted chlorophyll-a and phycocyanin fluorescence*

327

328
329 **Fig 4.** Spatio-temporal distribution of A) chlorophyll *a* concentration (µg.L^{-1}) and B) phycocyanin
330 fluorescence (r.u.)
331

332   Chl *a* concentration and phycocyanin fluorescence were not significantly different between the

333   southward and northward sailing directions (ANOVA, P>0.05). Chl *a* (Fig. 4A) showed significant

334   temporal (ANOVA, P <0.001) and spatial (ANOVA, P<0.001) variation. In April-May, a spring bloom

335   with a maximum chl *a* concentration of 12.7 µg.L^{-1} developed from the south towards the north. In July-

336   August, a summer bloom appeared only in the northern part of the transect with a maximum chl *a*

337   concentration of 13.5 µg.L^{-1}. During the rest of the studied period, chl *a* concentration stayed relatively

338   low (< 3 µg.L^{-1}) without any discernible spatial pattern. Phycocyanin fluorescence (Fig. 4B) was also

339   spatially (ANOVA, P<0.001) and temporally variable (ANOVA, P=0.01). A peak of phycocyanin

340   fluorescence with a maximum value of 0.9 (r.u.) was observed at the same time and location as a peak in

341   turbidity (appearing in July and only in the northern part of the transect). During the rest of the studied

342   period, phycocyanin levels remained low (<0.20).

343 *3.3. Maximum photochemical efficiency (F_v/F_m) and functional absorption cross-section of photosystems*

344 *II (σ_{PSII})*

345

346

347 **Fig 5.** Relationships between the maximum photochemical efficiency (F_v/F_m, relative units) measured at
348 458 and 593 nm (A) and between the functional absorption cross-section of photosystems II (σ_{PSII}, Å^2
349 quantum^{-1}) measured at 458 nm and 593 nm (B)

350

351   F_v/F_m(458), F_v/F_m(593), σ_{PSII}(458), σ_{PSII}(593) were not significantly different between the northward

352 and southward routes (ANOVA, P>0.05). While σ_{PSII}(593) was only significantly variable in time

353 (ANOVA, P<0.001), all other photosynthetic parameters were significantly variable in both space

354 (ANOVA, P<0.001) and time (ANOVA, P<0.001).

355   F_v/F_m(458) was always significantly higher than F_v/F_m(593) (Fig. 5A) (paired t-test, P<0.001).

356 F_v/F_m(458) ranged between 0.01 and 0.49 while F_v/F_m(593) ranged between 0.03 and 0.36. The temporal

357 variation of F_v/F_m(458) (Fig. 6A) differed between the different Baltic Sea areas with the highest and

358 lowest values of F_v/F_m(458) both recorded in the northern part of the transect (Northern Baltic Proper and

359 Western Gulf of Finland, from 58.4 to 60.0°N). In this area, high values of F_v/F_m(458) (>0.40) were

360 reached in April, mid-May (but just from 59.3 to 60.0 °N), at the beginning of June and at the beginning

361 of July. The lowest values were reached in early May and from mid-July to August. During the other

362 periods, F_v/F_m(458) varied between 0.30-0.35. In the central part of the transect (between 55.3 and 58.4

363 °N, including the Gotland basin and Bornholm basin), F_v/F_m(458) was high (>0.40) in April, from mid-

364 May to the beginning of June, from the last week of June to mid-July and at the end of August. Low

365 values of F_v/F_m(458) were obtained from the end of April to the first week of May (0.08-0.26), in mid-

366 June (0.25) around 57.8°N and at the end of July-beginning of August (0.16-0.30). The rest of the time

367 F_v/F_m(458) was around 0.30-0.35. In the southern part (Arkona basin and Mecklenburg bight, from 54.0

368 and 55.3 °N), F_v/F_m(458) reached its maximum value (0.38) at the end of April, showed several short

369 periods with low values (around 0.20) at the beginning of May, in July and in August, and a period with
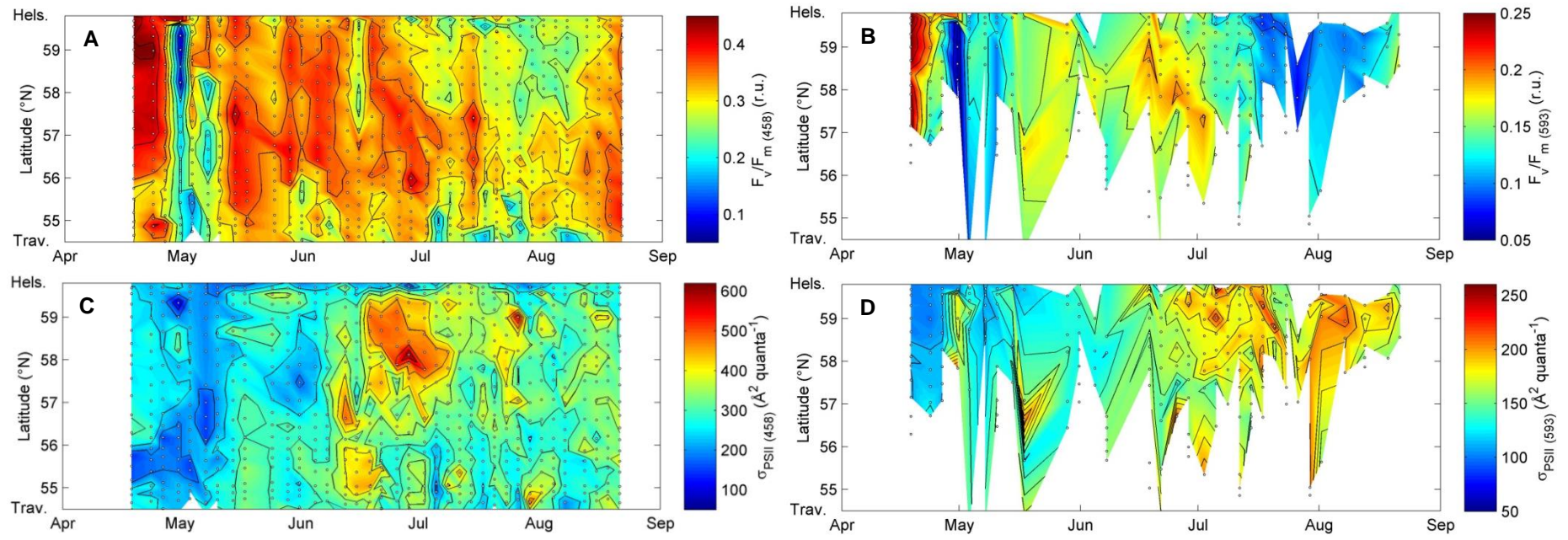
Fig 6. Spatio-temporal dynamics of the maximum photochemical efficiency measured at A) 458 nm ($F_v/F_m(458)$) and B) 593 nm ($F_v/F_m(593)$) and the functional absorption cross-section of photosystems II measured at C) 458 nm ($\sigma_{PSII}(458)$) and D) 593 nm ($\sigma_{PSII}(593)$). Note the different scales for $F_v/F_m(458)$, $F_v/F_m(593)$, $\sigma_{PSII}(458)$ and $\sigma_{PSII}(593)$

370 intermediate values (around 0.30) in May-June. $F_v/F_m(593)$ and $F_v/F_m(458)$ were significantly correlated

371 (r^2=0.60, P<0.001) (Fig. 5A) and showed similar spatio-temporal patterns of variation (Fig. 6A & B).

372 $\sigma_{PSII}(458)$ and $\sigma_{PSII}(593)$ were significantly different (paired t-test, P<0.001) and no significant

373 correlation was found between these parameters (Fig. 5B). $\sigma_{PSII}(458)$ ranged from 55 to 610 Å^2 quantum^{-1}

374 while $\sigma_{PSII}(593)$ ranged from 96 to 350 Å^2 quantum^{-1}. Temporal variation of $\sigma_{PSII}(458)$ (Fig. 6C) was

375 different between the different parts of the Baltic Sea. From 56.5 to 60.0°N, $\sigma_{PSII}(458)$ was low in April-

376 May and high from the end of June to July with the maximum value (610 Å^2 quantum^{-1}) observed at the

377 end of June. In the other part of the Baltic Sea (from 54.0 to 56.5°N), $\sigma_{PSII}(458)$ was also low in April-

378 May but the highest value (487 Å^2 quantum^{-1}) was reached in mid-June and the period with high values

379 was shorter. Like $\sigma_{PSII}(458)$, $\sigma_{PSII}(593)$ (Fig. 6D) was low in April. High $\sigma_{PSII}(593)$ values were, however,

380 observed later (from the end of June to the end of August) and over a longer period than high $\sigma_{PSII}(458)$

381 values. Also, in areas where data for both $\sigma_{PSII}(458)$ and $\sigma_{PSII}(593)$ were available, the spatial variability

382 of $\sigma_{PSII}(593)$ was lower than for $\sigma_{PSII}(458)$.

383 The relationship between F_v/F_m and σ_{PSII} (Fig. 7A,B) was complex and differed between both

384 excitation wavelengths (458 and 593 nm). Most of $F_v/F_m(458)$ values ranged between 0.20 and 0.40 and

385 were associated with $\sigma_{PSII}(458)$ values ranging between 140 and 600 Å^2 quantum^{-1} (Fig. 7A). A small

386 cluster of low $F_v/F_m(458)$ (<0.20) and low $\sigma_{PSII}(458)$ (between 54 and 300 Å^2 quantum^{-1}) values was also

387 visible. High $F_v/F_m(458)$ values (> 0.40) were associated with $\sigma_{PSII}(458)$ values around 200 Å^2 quantum^{-1}.

388 $F_v/F_m(593)$ varied widely (from 0.05 to 0.36) while most of the associated $\sigma_{PSII}(593)$ values were between

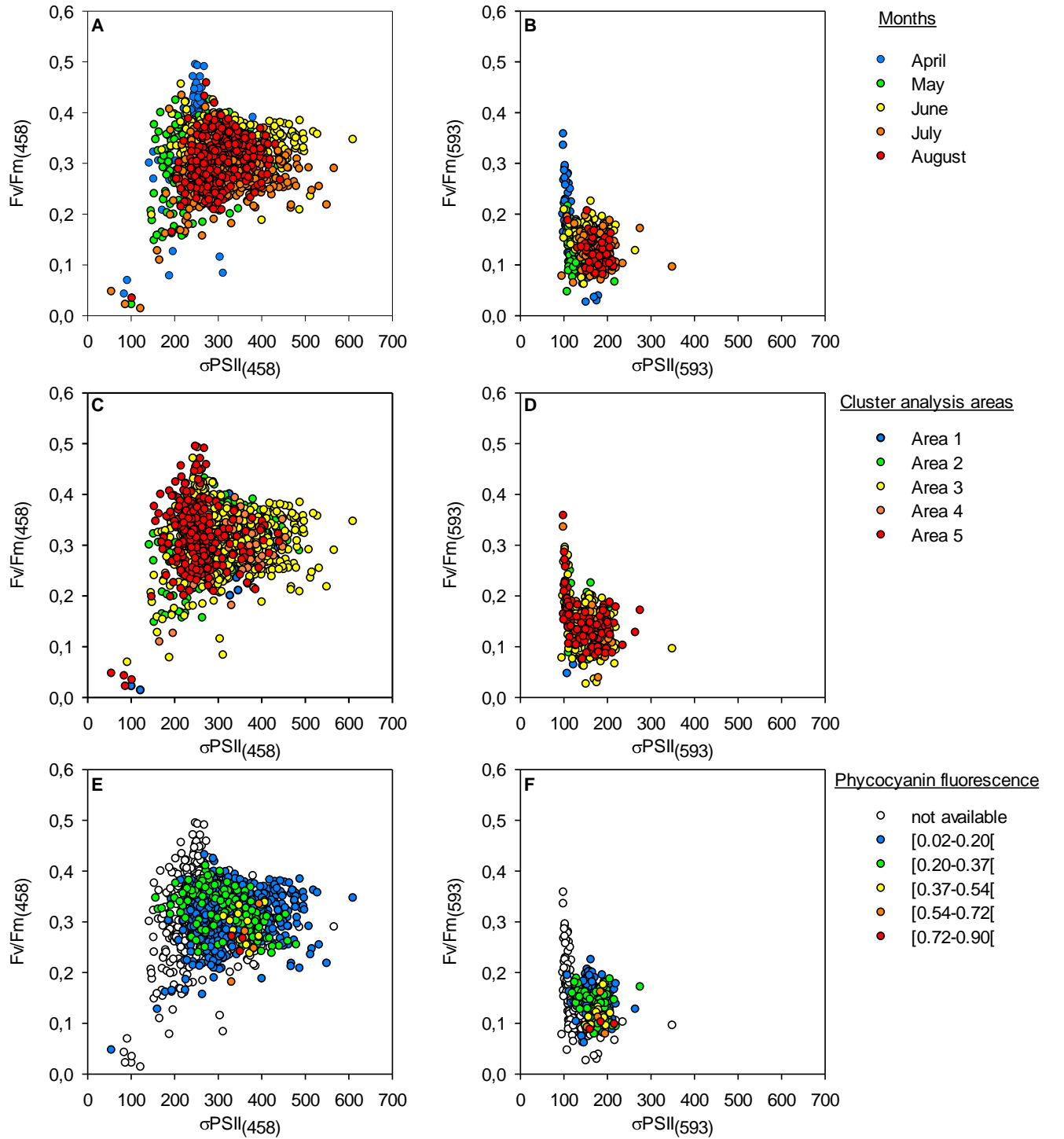389 100 and 200 Å^2 quantum^{-1} (Fig. 7B).

390

Fig. 7. Relationships between the maximum photochemical efficiency (F_v/F_m, relative units) and the functional absorption cross-section of photosystems II (σ_{PSII}, Å^2 quantum^{-1}) both measured at 458 nm (A,C,E) and 593 nm (B,D,F). The same dataset is presented in A,C,E for $F_v/F_m(458)$ vs. $\sigma_{PSII}(458)$ and B,D,F for $F_v/F_m(593)$ vs. $\sigma_{PSII}(593)$ but colours indicate: the observation month (A,B), cluster analysis areas (C,D) or phycocyanin fluorescence (E,F)

3.4. Relationships between physico-chemical factors, phytoplankton structure and photosynthetic

392 *parameters*

393

394
395 **Fig. 8.** Cluster analysis showing the results of sampling zones classification based on environmental
396 parameters and phytoplankton structure. Location of sampling zones is represented on Fig. 1
397

398 A cluster analysis based on environmental parameters, chl *a* and phycocyanin fluorescence

399 separated five significantly different (ANOSIM, R = 0.896, P =0.001) spatial regions along the ship route

400 as shown in Fig. 8. The first region included only the sampling zone 1 (Fig. 1) which corresponds to the

401 southernmost part of the transect (Mecklenburg Bight). This region was characterized by relatively high

402 salinity, higher temperature, lower CDOM concentration and low phycocyanin fluorescence. The second

403 cluster grouped the sampling zones 2 to 7 situated in Arkona Basin and Bornholm Basin and was

404 characterized by high salinity, high temperature, high E_d(PAR) and low turbidity. The third cluster

405 grouped the sampling zones 8 to 14 located in Gotland Basin and Northern Baltic Proper and comprised

406 the stations sampled during the night. Correspondingly, it is characterized by low E_d(PAR) as well as

407 intermediate levels of CDOM fluorescence and turbidity. The fourth cluster corresponded to zone 15 (i.e.

408 the mouth of the Gulf of Finland) characterized by low nutrient concentrations and periodically high

409 turbidity and phycocyanin fluorescence. The last cluster grouped zones 16 to 17 (i.e. the western Gulf of

410 Finland corresponding to the northernmost part of the transect) and was characterized by higher turbidity,

411 higher phycocyanin fluorescence, higher CDOM concentration and low salinity.

412 F_v/F_m(458), σ_{PSII}(458), F_v/F_m(593) and σ_{PSII}(593) were related to physico-chemical parameters and

413 phytoplankton structure using stepwise multiple linear regressions (Table 1). Different factors acted on

414 these photosynthetic parameters in each clustered region. In the first region, no significant relationship

415 was found with F_v/F_m(458) while σ_{PSII}(458) was negatively related to E_d(PAR). In the second region,

416 F_v/F_m(458) was negatively related to E_d(PAR) while σ_{PSII}(458) was influenced by both E_d(PAR) and

417 temperature. In these two first regions, insufficient data were available to relate F_v/F_m(593) and σ_{PSII}(593)

418 to environmental conditions. In the third region, $F_v/F_m(458)$ was related to temperature and PO_4^{3-}

419 concentration. $\sigma_{PSII}(458)$ was linked to $NO_2^-+NO_3^-$ concentration, $E_d(PAR)$ and CDOM fluorescence.

420 $F_v/F_m(593)$ was negatively related to both temperature and turbidity and $\sigma_{PSII}(593)$ was negatively related

421 to CDOM fluorescence. In the fourth region, $F_v/F_m(458)$ was negatively related to temperature and

422 turbidity. No significant relationship was found with $\sigma_{PSII}(458)$. $F_v/F_m(593)$ and $\sigma_{PSII}(593)$ were

423 respectively negatively and positively correlated with temperature. In the third and fourth region, turbidity

424 was positively related to phycocyanin fluorescence. Consequently, the influence of turbidity on

425 photosynthetic parameters must be read as a combined relation to turbidity and phycocyanin fluorescence.

426 In the northernmost region (area 5), $F_v/F_m(458)$ was negatively related to temperature and turbidity and

427 positively related to phycocyanin fluorescence while $\sigma_{PSII}(458)$ was related to phycocyanin fluorescence,

428 temperature and turbidity. $F_v/F_m(593)$ was influenced by temperature and no significant relationship was

429 found with $\sigma_{PSII}(593)$.

430   The different modes of variation observed in the relationships between $F_v/F_m(458)$ and $\sigma_{PSII}(458)$

431 and between $F_v/F_m(593)$ and $\sigma_{PSII}(593)$ could not be related to either month of observation (Fig. 7A,B),

432 sea areas defined by the cluster analysis (Fig. 7C,D), or phycocyanin fluorescence intensity (Fig. 7E,F).

433

Table 1: Stepwise multiple linear regressions relating the maximum photochemical efficiency (F_v/F_m) and the functional absorption cross-section of photosystems II (σ_{PSII}) measured at 458 and 593 nm to environmental factors and phytoplankton composition

Regression equation	r^2	F	P	n
Area 1				
$\sigma_{PSII}(458) = 401.11 - 0.21\ E_d(PAR)$	0.33	8.43	0.012	16
Area 2				
$F_v/F_m(458) = 0.34 - 2.90E\text{-}05\ E_d(PAR)$	0.08	25.89	< 0.001	207
$\sigma_{PSII}(458) = 444.49 - 0.05\ E_d(PAR) - 4.84$ TEMP.	0.39	67.25	< 0.001	207
Area 3				
$F_v/F_m(458) = 0.37 - 0.01$ TEMP. $+ 0.47\ PO_4^{3-}$	0.45	20.75	< 0.001	49
$\sigma_{PSII}(458) = 519.39 - 846.12\ NO_2^-+NO_3^- - 0.13\ E_d(PAR) - 456.25$ CDOM	0.31	5.37	0.026	30
$F_v/F_m(593) = 0.24 - 4.72E\text{-}03$ TEMP. $- 5.02E\text{-}02$ TURB.	0.60	127.54	< 0.001	169
$\sigma_{PSII}(593) = 191.01 - 143.66$ CDOM	0.46	11.30	0.006	13
Area 4				
$F_v/F_m(458) = 0.44 - 5.27E\text{-}03$ TEMP. $- 4.27E\text{-}03$ TURB.	0.49	20.99	< 0.001	43
$F_v/F_m(593) = 0.22 - 5.50E\text{-}03$ TEMP.	0.54	31.41	< 0.001	27
$\sigma_{PSII}(593) = 133.01 + 2.88$ TEMP.	0.23	8.91	0.006	27
Area 5				
$F_v/F_m(458) = 0.42 - 3.74E\text{-}03$ TEMP. $- 0.12$ TURB. $+ 0.48$ PHYCO.	0.58	31.36	< 0.001	67
$\sigma_{PSII}(458) = 216.42 + 524.76$ PHYCO $+ 6.97$ TEMP. $- 103.77$ TURB.	0.19	6.82	< 0.001	77
$F_v/F_m(593) = 0.22 - 5.99E\text{-}03$ TEMP.	0.36	21.14	< 0.001	37

r^2 = adjusted coefficient of multiple determination (in %), TEMP. = temperature, PHYCO. = phycocyanin fluorescence, TURB. = turbidity

434

435

436

437

438

439 **4. Discussion**

440 *4.1. Dynamics and control of photosynthetic parameters measured using blue excitation (458 nm)*

441

442 $F_v/F_m(458)$ and $\sigma_{PSII}(458)$ values were in accordance with FRRf-based ST values of F_v/F_m and σ_{PSII}

443 that can be expected for mixed phytoplankton communities containing cyanobacteria when the

444 measurements are made using a FRRF equipped with blue excitation (Raateoja et al., 2004b; Suggett et

445 al., 2009) and fell within the range of values found previously in the Baltic Sea (Raateoja et al., 2004a;

446 Raateoja, 2004).

447 $F_v/F_m(458)$ had complex spatio-temporal dynamics and showed different degree of variation in the

448 different areas of the Baltic Sea. This variability was, however, not directly correlated with the dominant

449 gradients in physico-chemical parameters of the Baltic Sea. Also no relationship was found between the

450 spatial distribution of $F_v/F_m(458)$ and the period of the day at which areas were sampled (i.e. during day

451 or night time). The control of $F_v/F_m(458)$ spatial distribution seemed to be multivariate and related to the

452 different associations of environmental conditions characterizing the different areas of the Baltic Sea

453 which influenced $F_v/F_m(458)$ in different ways. In the southern part of the transect, $E_d(PAR)$ was the most

454 influential factor while temperature variations and either nutrient availability in the center part or turbidity

455 and phycocyanin fluorescence in the northern part influenced $F_v/F_m(458)$.

456 Temporal variability of $F_v/F_m(458)$ generally exceeded spatial variability. Temporal variations of

457 $F_v/F_m(458)$ did not follow an obvious seasonal cycle. However, each phytoplankton bloom was followed

458 by a period of very low $F_v/F_m(458)$ i.e. in May along the whole route and at the end of July-beginning of

459 August in the northern part. To our knowledge, few studies have focused on the temporal variability of

460 F_v/F_m at seasonal scale in temperate northern marine systems (Aiken et al., 2004; Houliez et al., 2013;

461 Houliez et al., 2015; Napoléon et al., 2013; Napoléon et al., 2012). All carried out in the English Channel,

462 these studies reported differing results. Aiken et al. (2004) and Houliez et al. (2013; 2015) indicated that

463 F_v/F_m varied at weekly scale without any evidence of a seasonal cycle. Napoléon et al. (2013; 2012)

464 studied the dynamics of F_v/F_m along two transects crossing the English Channel and found different

465 temporal variability between the French and English coasts. Along the French coast, F_v/F_m stayed

466 relatively high and stable throughout the year while from the English coast to the central part of each

467 transect, F_v/F_m followed a seasonal cycle with high values in autumn-winter and low values in spring-

468 summer. The high temporal variability of $F_v/F_m(458)$ without evidence of a seasonal pattern seen in the

469 current study is similar to the results of Aiken et al. (2004) and Houliez et al. (2013; 2015). Additionally,

470 reflecting the results of Houliez et al. (2013; 2015), each phytoplankton bloom was followed by a period

471 with low F_v/F_m values. They are also consistent with the results of Seppälä (2009) showing that in the

472 Gulf of Finland, the effective photochemical efficiency of PSII (F_q'/F_m') measured at 470 nm with a

473 FAST[tracka], varied without evidence of a seasonal pattern and dropped after each phytoplankton bloom.

474 These low $F_v/F_m(458)$ values observed after each bloom could be the result of nutrient stress

475 following peak growth, but could also have been influenced by the presence of cyanobacteria within the

476 phytoplankton community. It is known that F_v/F_m values for cyanobacteria can be as low as 0.10 to 0.40

even in absence of physiological stress when the measurements are made using a FRRF equipped with a blue excitation light (Suggett et al., 2009). Additionally, while it has been shown that nutrient starvation or light stress result in a simultaneous decrease of F_v/F_m and increase of σ_{PSII} (Geider et al., 1993; Kolber et al., 1988; Ragni et al., 2008; Vassiliev et al., 1994), this pattern was not observed here. Indeed, during these periods, $F_v/F_m(458)$ decreased without simultaneous increase of $\sigma_{PSII}(458)$ while a rise of $\sigma_{PSII}(593)$ was observed. The phycobilipigments cyanobacteria use to harvest light for photosynthesis in the green-orange part of the visible spectrum form the best explanation for increased $\sigma_{PSII}(593)$ because this part of the spectrum is little used by the diatoms and dinoflagellates dominating the algal community in the Baltic Sea (Johnsen and Sakshaug, 2007; Seppälä et al., 2005; Simis et al., 2012). However, because $F_v/F_m(593)$ decreased at the same time, it cannot be ruled out that physiological stress affected cyanobacteria. It is, however, promising that the rapid *in situ* observation of photophysiological properties can now be used to strategically trigger water sampling from ships-of-opportunity, allowing detailed study of these key moments in phytoplankton succession.

Dynamics of $\sigma_{PSII}(458)$ presented some differences between the southern and northern parts of the Baltic Sea. In the northern part, $\sigma_{PSII}(458)$ values stayed high during a longer period than in the south which is consistent with higher nutrient concentrations in the Gulf of Finland fueling longer blooms (Groetsch et al., 2016). However, in both areas, $\sigma_{PSII}(458)$ started to increase from May and the highest values of $\sigma_{PSII}(458)$ were reached in June i.e. during the period of the year when light availability and temperature seasonally increase. Multiple linear regressions confirmed the influence of $E_d(PAR)$ and temperature on $\sigma_{PSII}(458)$ dynamics but the relationship was not always positive, suggesting a more complex control of $\sigma_{PSII}(458)$. Raateoja et al. (2004a) found a similar increase of the functional absorption cross-section of photosystems II under actinic light (σ_{PSII}') from May to summer in the northern part of the Baltic Sea (Gulf of Finland). Their results showed that σ_{PSII}' followed the same patterns of variation as the chlorophyll a specific absorption (a_{ph}^*) that was influenced by seasonal successions in phytoplankton community structure. σ_{PSII}' and a_{ph}^* were thus low when phytoplankton biomass was high and dominated by large phytoplankton cells and high during the clear-water phase with low biomass and a dominance of picoplankton. Taxonomic dependence of σ_{PSII} have been observed in different systems and have been primarily explained by the differences existing in the concentration, type and arrangement of pigments within the PSII antenna in addition to the associated PSII reaction center (RCII) concentration (Moore et al., 2006; Suggett et al., 2004; Suggett et al., 2009). A size dependence of σ_{PSII} with higher values for smaller phytoplankton cells has also been reported by Suggett et al. (2009). Consequently, in addition to $E_d(PAR)$ and temperature, $\sigma_{PSII}(458)$ dynamics were likely influenced by seasonal changes in phytoplankton community structure.

The relationship between $F_v/F_m(458)$ and $\sigma_{PSII}(458)$ was complex and showed no straightforward trend. Analyzing different data sets collected on laboratory grown monocultures and *in situ* in different ecosystems using a FRRF equipped with a blue excitation light (478 nm), Suggett et al. (2009) showed that σ_{PSII} and F_v/F_m were inversely related and that the trend of this relationship was variable between data sets but also taxon-dependent. Results from laboratory experiments showed that the F_v/F_m versus σ_{PSII}

relationship can follow two modes of variations. F_v/F_m versus σ_{PSII} relationship measured on algae presented a gradual decrease of F_v/F_m with simultaneous increase of σ_{PSII} (from high-F_v/F_m, low-σ_{PSII} to low-F_v/F_m, high-σ_{PSII}) while this relationship was much steeper for cyanobacteria (Suggett et al., 2009). The unstructured relationship between $F_v/F_m(458)$ and $\sigma_{PSII}(458)$ may thus reflect a mixture of these two modes of variation (cyanobacteria and algae) as would be expected given the composition of phytoplankton communities in the Baltic Sea. Similar relationships have been observed with the AMT 15 data set collected during trans-Atlantic (North to South) cruises and have been related to the presence of cyanobacteria (Suggett et al., 2009). Indeed, during the AMT 15 cruises, communities with low cyanobacteria dominance (low zeaxanthin: chlorophyll ratios) displayed a similar mode of variation as the one found for algae during laboratory experiments, while communities with relatively high zeaxanthin concentration, indicating an increased dominance of *Synechococcus sp.*, were associated with a group of observations with low σ_{PSII} and low F_v/F_m values. Although this explanation is satisfying, no relationship was found between the trends observed in the $F_v/F_m(458)$ and $\sigma_{PSII}(458)$ relationship and phycocyanin fluorescence. It is possible that phycocyanin fluorescence measurements did not capture some changes in cyanobacterial community composition because, even though phycocyanin fluorescence has been shown to accurately describe the bloom forming filamentous cyanobacteria that dominate phytoplankton community in summer (Seppälä et al., 2007), some picocyanobacteria present in the Baltic Sea (e.g. *Synechococcus sp.*), are rich in phycoerythrin rather than phycocyanin (Haverkamp et al., 2009). Once more, however, the wide range of σ_{PSII} and F_v/F_m responses to physiological stress cannot be excluded as another possible explanation (Geider et al., 1993; Herrig and Falkowski, 1989; Kolber et al., 1988). It has been shown that for a given species, σ_{PSII} increases and F_v/F_m decreases in response to stressors like nutrient starvation, photoinhibition and/or UV radiation (Ragni et al., 2008; Vassiliev et al., 1994). Moreover, Suggett et al. (2009) observed that in case of stress due to nutrient limitation, the modes of variation in the relationship between σ_{PSII} and F_v/F_m looks like the taxon-dependent relationship observed for algae. Consequently, the different modes of variation observed in the relationship between $F_v/F_m(458)$ and $\sigma_{PSII}(458)$ may well be caused by both environmental conditions and phytoplankton composition.

4.2 Measurements under amber excitation (593 nm)

Spatio-temporal dynamics of $F_v/F_m(458)$ and $F_v/F_m(593)$ were similar and both were influenced by temperature and turbidity. This suggests that the adjustment of the maximum photochemical efficiency in response to variations in environmental factors was similar for the different groups (algae vs. cyanobacteria) present within phytoplankton community. To date, studies on F_v/F_m resulting from different excitation wavebands are very scarce. To our best knowledge, thus far only Ralph and coworkers (unpublished data cited in Robinson et al. (2014)) reported on cyanobacterial influence in field measurements of F_v/F_m using a fluorometer equipped with excitation lights emitting at two wavelengths (blue and red). Their data acquired at an oligotrophic station in the Tasman Sea shows that F_v/F_m values measured under red excitation were lower than those measured under blue excitation. Their explanation

553 for this difference is that the blue channel measures the fluorescence signal from the total phototrophic

554 community while the red channel is indicative of the cyanobacterial part. The differences between

555 $F_v/F_m(458)$ and $F_v/F_m(593)$ observed in the Baltic Sea should be interpreted in the same way because the

556 593 nm excitation window was chosen to saturate the absorption tails of phycocyanin (maximum around

557 615 nm) and phycoerythrin (maximum around 560 nm). Nevertheless, the season of significant signal

558 from amber light excitation in the Baltic Sea is relatively short, limiting the scope of this assessment to

559 the most prominent dynamics. Most importantly, the fact that increased $\sigma_{PSII}(593)$ coincided with an

560 increase in phycocyanin fluorescence indicates that the instrument is sensitive to the cyanobacterial part

561 of the community. However, more detailed taxonomic information than currently collected will be

562 required to explore relationships between $F_v/F_m(593)$, the proportion of cyanobacteria vs. algae within the

563 phytoplankton community, and stressors like nutrients or light.

564     $\sigma_{PSII}(593)$ was consistently lower than $\sigma_{PSII}(458)$. This difference in $\sigma_{PSII}(593)$ values in comparison

565 to $\sigma_{PSII}(458)$ is in itself not a quantitative measure of the role of cyanobacteria in community light

566 harvesting. Indeed, differences in σ_{PSII} values are to be expected when measurements are made at

567 different wavelengths, because the efficiency with which PSII is receives energy from lights absorbed at

568 different wavelengths and subsequently emits fluorescence depends on the type and arrangement of

569 pigments within the PSII antennae (Johnsen and Sakshaug, 2007; MacIntyre et al., 2010). Suggett et al

570 (2009) have for example observed that the cyanobacterium *Synechococcus sp*. WH7803 exhibits a value

571 of σ_{PSII} five times higher after excitation at 550 nm than at 478 nm because of its specific pigment

572 organization into phycobilisomes. In contrast, differences in the spatio-temporal dynamics of $\sigma_{PSII}(458)$

573 and $\sigma_{PSII}(593)$ can be a good indication of the role of phytoplankton community composition because for

574 a same species, dynamics of σ_{PSII} measured at both wavelengths should be similar while this will not be

575 the case with a mixture of species with different σ_{PSII}. In our study, spatio-temporal dynamics of

576 $\sigma_{PSII}(458)$ and $\sigma_{PSII}(593)$ showed the most prominent differences in summer between the end of June and

577 the end of August when filamentous cyanobacteria bloomed. Although taxonomic data are too scarce to

578 untangle physiological responses from dynamics in the algal vs. cyanobacterial parts of the community,

579 this pattern is expected and marks a clear improvement of the dual light source approach over previous

580 attempts to chart photophysiological parameters in the Baltic Sea (Raateoja et al., 2004b). At present, the

581 deep analysis of the factors governing $\sigma_{PSII}(593)$ did not reveal any significant trends. Additional

582 continuous measurements, particularly during periods of rapid changes in environmental conditions,

583 should help to reveal such controls on the presumed cyanobacterial contribution to primary production.

584   From a technical point of view, most of the time, fluorescence excitation with amber light was

585 subject to low signal strength because pigments that absorb in this waveband occurred in relatively low

586 concentrations, and with a strong seasonal dynamic. Gaps in amber-excited fluorescence parameters thus

587 occurred when induction curves were of insufficient good quality to fit the KPF model and to extract the

588 photosynthetic parameters. Alternative causes for gaps in the retrieval of these parameters, such as

589 insufficient detector sensitivity or insufficient excitation intensity, can be ruled out. Maximum amber

590 excitation light intensity (65,000 µmol photons m^{-2} s^{-1}) should be more than adequate to saturate PSII and

591 the detector is in both cases centred on red PSII fluorescence. However, the stokes shift from blue

592 excitation to red fluorescence allows good separation of excitation light and emitted fluorescence using

593 optical filters, whereas cross-talk between amber excitation and red fluorescence is more significant. This

594 cross-talk is calibrated using weekly instrument characterization on a filtered ultrapure water sample. In

595 the absence of any particles, this signal is flat and can be subtracted from each measurement. In the

596 presence of small particles, the response would be homogeneous within the light path. In the presence of

597 mixed particle populations and more so when larger particles are interspersed with smaller particles we

598 would expect the signal to be most variable between flashlets. If, in addition, F_v/F_m is low, scatter in the

599 signal may far exceed any observable rise in fluorescence (F_v). A solution to this problem, which has been

600 exercised many times in the past with single-channel FRRF, is to average the results of multiple induction

601 curves, which will reduce the noise and reveal the systematic rise in Fv for a given sample. During this

602 initial testing campaign, averaging was not programmed, in order to establish a threshold for usability. In

603 future, we recommend averaging at least five consecutive measurements, observing relatively long (1-s)

604 pauses between repeated measurements. The above considerations and adaptations of the measurement

605 protocol would likely result in better resolution of periods where the fluorescence signals are already low.

606 Phytoplankton succession and population dynamics are therefore still the dominant cause of gaps in the

607 data. When measurements are made on a group lacking pigments that absorb in a particular waveband,

608 the fluorescence signal may be too low to be detected or the induction curve obtained with this excitation

609 wavelength will not necessarily reach saturation. This is already accepted in fluorescence-based

610 measurements of phytoplankton photosynthesis when it was shown that cyanobacteria do not always

611 reach saturation under blue excitation (Raateoja et al., 2004; Suggett et al., 2009). With multiwavelength

612 fluorometers, like the FFL-40, the same phenomenon can occur under excitation with the others colours.

613 For instance, excitation of diatoms or green algae with blue excitation light will provide a good induction

614 curve while saturation might not be reached with amber excitation light. Additionally, the group with the

615 highest sensitivity for a particular excitation waveband may out-fluoresce the other groups and to an

616 extent mask their fluorescence signal.

617

618 **5**. **Conclusions**

619

620   The present study reports for the first time, time series of F_v/F_m and σ_{PSII} acquired at basin scale

621 using a flow-through FRRF equipped with two excitation channels (458 and 593 nm), which marks a step

622 towards better integration of autonomous assessment of phytoplankton photophysiological conditions in

623 phytoplankton communities that are naturally diverse in their share of algae and cyanobacteria.

624   Patterns of spatio-temporal variation of the maximum photochemical efficiency (F_v/F_m) were found

625 to be similar after excitation at 458 nm or 593 nm suggesting that the adjustment of F_v/F_m in response to

626 variations in environmental factors was similar for the different groups (algae vs. cyanobacteria) present

627 within phytoplankton community. In contrast, dynamics of the functional absorption cross-section of

628 photosystems II (σ_{PSII}) were dependent on the light excitation waveband used to excite PSII particularly

629 during the cyanobacteria dominated summer. The F_v/F_m and σ_{PSII} observations showed different responses

630 between Baltic Sea areas governed by different conditions mainly in term of light regime experienced

631 along the ship route, nutrient availability and temperature. However, even though the Baltic is

632 characterized by several physico-chemical gradients no gradient was observed in F_v/F_m and σ_{PSII} spatial

633 distribution suggesting complex interactions between biotic and abiotic controls.

634 To better understand the role that phytoplankton community structure (in particular changes in

635 cyanobacteria vs. algae proportions within community) plays in dynamics of F_v/F_m and σ_{PSII} measured at

636 different wavelengths, future studies should associate FRRF measurements with more detailed taxonomic

637 data (microscopy, HPLC pigments measurements or flow cytometry). Furthermore, the measurement of

638 fluorescence light curves associated with the increased sensitivity of FRRF to the whole phytoplankton

639 community due to inclusion of multiple excitation light sources should contribute to a better

640 understanding of the role of cyanobacteria in phytoplankton primary production dynamics.

641

651

652

653

654

655

656 **References**

657

658 Aiken, J., Fishwick, J., Moore, G., Pemberton, K., 2004. The annual cycle of phytoplankton
659 photosynthetic quantum efficiency, pigment composition and optical properties in the western English
660 Channel. J. Mar. Biol. Assoc. U. K. 84, 301-313.
661 Bianchi, T.S., Engelhaupt, E., Westman, P., Andrén, T., Rolff, C., Elmgren, R., 2000. Cyanobacteria
662 blooms in the Baltic Sea: Natural or human-induced? Limnol Oceanogr 45, 716-726.
663 Brzezinski, M.A., 1985. The Si:C:N ratio of marine Diatoms: interspecific variability and the effect of
664 some environmental variables. J Phycol 21, 347-357.
665 Clarke, K.R., Warwick, R.M., 2001. Change in marine communities: an approach to statistical analysis
666 and interpretation, 2nd edition. PRIMER-E, Plymouth, UK, 172 pp.
667 Cloern, J.E., 1996. Phytoplankton bloom dynamics in coastal ecosystems: A review with some general
668 lessons from sustained investigation of San Francisco Bay, California. Rev Geophys 34, 127-168.
669 Cullen, J.J., Davis, R.F., 2003. The blank can make a big difference in oceanographic measurements.
670 Limnology & Oceanography Bulletin 12, 29-35.

671   Falkowski, P.G., Raven, J.A., 2007. Aquatic Photosynthesis, 2nd edition. Blackwell Science. 500 pp.

672   Gaarder, T., Gran, H.H., 1927. Production of plankton in the Oslo Fjord. Rapports et Procès-Verbaux des

673   Réunions. Conseil Permanent International pour l'Exploration de la Mer 42, 1-48.

674   Geider, R.J., Delucia, E.H., Falkowski, P.G., Finzi, A.C., Philip Grime, J., Grace, J., Kana, T.M., La

675   Roche, J., Long, S.P., Osborne, B.A., Platt, T., Colin Prentice, I., Raven, J.A., Schlesinger, W.H.,

676   Smetacek, V., Stuart, V., Sathyendranath, S., Thomas, R.B., Vogelmann, T.C., Williams, P., Ian

677   Woodward, F., 2001. Primary productivity of planet earth: Biological determinants and physical

678   constraints in terrestrial and aquatic habitats. Global Change Biology 7, 849-882.

679   Geider, R.J., La Roche, J., Green, R.M., Olaizola, M., 1993. Response of the photosynthetic apparatus of

680   *Phaeodactylum tricornutum* (Bacillariophyceae) to nitrate, phosphate, or iron starvation. J Phycol 29,

681   755-766.

682   Groetsch, P.M.M., Simis, S.G.H., Eleveld, M.A., Peeters, S.W.M., 2014. Cyanobacterial bloom detection

683   based on coherence between ferrybox observations. J Mar Syst 140 Part A, 50-58.

684   Groetsch, P.M.M., Simis, S.G.H., Eleveld, M.A., Peters, S.W.M., 2016. Spring blooms in the Baltic Sea

685   have weakened but lengthened from 2000 to 2014. Biogeosciences Discussions bg-2015-636.

686   Hällfors, H., Backer, H., Leppänen, J.M., Hällfors, S., Hällfors, G., Kuosa, H., 2013. The northern Baltic

687   Sea phytoplankton communities in 1903-1911 and 1993-2005: a comparison of historical and modern

688   species data. Hydrobiologia 707, 109-133.

689   Hama, T., Miyazaki, T., Ogawa, Y., Iwakuma, T., Takahashi, M., Otsuki, A., Ichimura, S., 1983.

690   Measurement of photosynthetic production of a marine phytoplankton population using a stable ^{13}C

691   isotope. Mar Bio 73, 31-36.

692   Haverkamp, T.H.A., Schouten, D., Doeleman, M., Wollenzien, U., Huisman, J., Stal, L.J., 2009. Colorful

693   microdiversity of *Synechococcus* strains (picocyanobacteria) isolated from the Baltic Sea. The ISME

694   Journal 3, 397-408.

695   HELCOM, 2003. The Baltic Marine Environment 1999-2002. Baltic Sea Environment Proceedings 87,

696   48 pp.

697   Herrig, R., Falkowski, P., 1989. Nitrogen limitation in *Isochrysis galbana* (Haptophyceae). I.

698   Photosynthetic energy conversion and growth efficiencies. J Phycol 25, 462-471.

699   Houliez, E., Lizon, F., Artigas, L.F., Lefebvre, S., Schmitt, F.G., 2013. Spatio-temporal variability of

700   phytoplankton photosynthetic activity in a temperate macrotidal ecosystem: a novel use of Pulse

701   Amplitude Modulated (PAM) fluorometry. Estuar Coast Shelf Sci 129, 37-48.

702   Houliez, E., Lizon, F., Lefebvre, S., Artigas, L.F., Schmitt, F.G., 2015. Phytoplankton photosynthetic

703   activity dynamics in a temperate macrotidal ecosystem (the Strait of Dover, eastern English Channel):

704   time scales of variability and environmental control. J Mar Syst 147, 61-75.

705   Johnsen, G., Sakshaug, E., 2007. Biooptical characteristics of PSII and PSI in 33 species (13 pigment

706   groups) of marine phytoplankton, and the relevance for pulse amplitude-modulated and fast-repetition-

707   rate fluorometry. J Phycol 43, 1236-1251.

708   Kolber, Z., Zehr, J., Falkowski, P., 1988. Effects of growth irradiance and nitrogen limitation on

709   photosynthetic energy conversion in Photosystem II. Plant Physiol. 88, 923-929.

710   Kolber, Z.S., Prasil, O., Falkowski, P.G., 1998. Measurements of variable chlorophyll fluorescence using

711   fast repetition rate techniques: Defining methodology and experimental protocols. Biochim Biophys Acta

712   - Bioenergetics 1367, 88-106.

713   Kromkamp, J., Forster, R., 2003. The use of variable fluorescence measurements in aquatic ecosystems:

714   differences between multiple and single turnover measuring protocols and suggested terminology. Eur J

715   Phycol 38, 103-112.

716   Kromkamp, J.C., Dijkman, N.A., Peene, J., Simis, S.G.H., Gons, H.J., 2008. Estimating phytoplankton

717   primary production in Lake IJsselmeer (The Netherlands) using variable fluorescence (PAM-FRRF) and

718   C-uptake techniques. Eur J Phycol 43, 327-344.

719   Lawrenz, E., Silsbe, G., Capuzzo, E., Ylostalo, P., Forster, R.M., Simis, S.G.H., Prasil, O., Kromkamp,

720   J.C., Hickman, A.E., Moore, C.M., Forget, M.H., Geider, R.J., Suggett, D.J., 2013. Predicting the

721   Electron Requirement for Carbon Fixation in Seas and Oceans. PLoS ONE 8, e58137.

722   Lehtonen, K., Schiedek, D., 2006. Monitoring biological effects of pollution in the Baltic Sea: Neglected

723   but still wanted? Mar. Pollut. Bull. 53, 377-386.

724   Leppänen, J.M., Rantajärvi, E., Maunumaa, M., Larinmaa, M., Pajala, J., 1994. Unattended algal

725   monitoring system - a high resolution method for detection of phytoplankton blooms in the Baltic Sea.

726   Proceeding of OCEANS94, 461-463.

727 MacIntyre, H.L., Lawrenz, E., Richardson, T.L., 2010. Taxonomic discrimination of phytoplankton by
728 spectral fluorescence, in: Suggett D.J. *et al*. (Ed.), Chlorophyll a Fluorescence in Aquatic Sciences :
729 Methods and Applications, pp. 129-169.
730 Marra, J., 2002. Approaches to the Measurement of Plankton Production, in: Williams, P.J.l.B., Thomas,
731 D.N., Reynolds, C.S. (Eds.), Phytoplankton Productivity : Carbon assimilation in marine and freshwater
732 ecosystems. Blackwell Science, Oxford, pp. 78-108.
733 Mauzerall, D., Greenbaum, N.L., 1989. The absolute size of a photosynthetic unit. Biochim Biophys Acta
734 974, 119-140.
735 Montford, K., 1969. Measuring dissolved oxygen as an indicator of primary productivity. Chesap Sci 10,
736 327-330.
737 Moore, C.M., Suggett, D.J., Hickman, A.E., Kim, Y.N., Tweddle, J.F., Sharples, J., Geider, J.R.,
738 Holligan, P., 2006. Phytoplankton photoacclimation and photoadaptation in response to environmental
739 gradients in shelf sea. Limnol Oceanogr 51, 936-949.
740 Müller, A.M., Wasmund, N., 2003. Photophysiology of Surface Phytoplankton Communities in a
741 Transect from the Mouth of the Peene-Strom to the Arkona Sea (Baltic). International Review of
742 Hydrobiology 88, 482-497.
743 Napoléon, C., Fiant, L., Raimbault, V., Claquin, P., 2013. Study of dynamics of phytoplankton and
744 photosynthetic parameters using opportunity ships in the western English Channel. J Mar Syst 128, 146-
745 158.
746 Napoléon, C., Raimbault, V., Fiant, L., Riou, P., Lefebvre, S., Lampert, L., Claquin, P., 2012.
747 Spatiotemporal dynamics of physicochemical and photosynthetic parameters in the central English
748 Channel. J Sea Res 69, 43-52.
749 Olli, K., Klais, R., Tamminen, T., Ptacnik, R., Andersen, T., 2011. Long term changes in the Baltic Sea
750 phytoplankton community. Boreal Environment Research 16, 3-14.
751 Raateoja, M., Seppälä, J., Kuosa, H., 2004a. Bio-optical modelling of primary production in the SW
752 Finnish coastal zone, Baltic Sea: fast repetition rate fluorometry in Case 2 waters. Mar Ecol Prog Ser 267,
753 9-26.
754 Raateoja, M., Seppälä, J., Ylöstalo, P., 2004b. Fast repetition rate fluorometry is not applicable to studies
755 of filamentous cyanobacteria from the Baltic Sea. Limnol Oceanogr Methods 49, 1006-1012.
756 Raateoja, M.P., 2004. Fast repetition rate fluorometry (FRRF) measuring phytoplankton productivity: A
757 case study at the entrance to the Gulf of Finland, Baltic Sea. Boreal Environment Research 9, 263-276.
758 Ragni, M., Airs, R., Leonardos, N., Archer, S., Geider, R.J., 2008. Photoinhibition of PSII in *Emiliania*
759 *huxleyi* (Haptophyta) under high light stress : the roles of photoacclimation, photoprotection and
760 photorepair. J Phycol 44, 670-683.
761 Rantajärvi, E., Flinkman, J., Ruokanen, L., Hällfors, S., Stipa, T., Suominen, T., Kaitala, S., Maunula, P.,
762 Fleming, V., Lips, U., London, L., Vepsäläinen, J., Nyman, E., Neuvonen, S., Suominen, T., Kankaanpää,
763 H., Seppälä, J., Perttilä, M., Raateoja, M., Haahti, H., 2003. Alg@line in 2003: 10 years of innovative
764 plankton monitoring and research an operational information service in the Baltic Sea. Technical Report.
765 Finnish Institute of Marine Research.
766 Redfield, A.C., 1934. On the proportions of organic derivations in sea water and their relation to the
767 composition of plankton, in: Daniel, R.J. (Ed.), James Johnstone Memorial Volume. University Press of
768 Liverpool, pp. 177-192.
769 Renk, H., Ochocki, S., 1998. Photosynthetic rate and light curves of phytoplankton in the southern Baltic.
770 Oceanologia 40, 331-344.
771 Robinson, C., Suggett, D.J., Cherukuru, N., Ralph, P.J., Doblin, M.A., 2014. Performance of Fast
772 Repetition Rate fluorometry based estimates of primary production in coastal waters. J Mar Syst 139,
773 299-310.
774 Ruokanen, L., Kaitala, S., Fleming, V., Maunula, P., 2003. Alg@line: joint operational unattended
775 phytoplankton monitoring in the Baltic Sea. Elsevier Oceanography Series 69, 519-522.
776 Rydberg, L., AErtebjerg, G., Edler, L., 2006. Fifty years of primary production measurements in the
777 Baltic entrance region, trends and variability in relation to land-based input of nutrients. J Sea Res 56, 1-
778 16.
779 Sall, J., Creighton, L., Lehman, A., 2007. JMP Start Statistics: A Guide to Statistics and Data Analysis
780 Using JMP. 4th Edition. Cary, NC: SAS Institute Inc. 607 pp.
781 Scherrer, B., 2007. Biostatistique, Volume 1, 2e édition. Gaëtan Morin éditeur. 816 pp.

782 Schreiber, U., Klughammer, C., Kolbowski, J., 2012. Assessment of wavelength-dependent parameters of
783 photosynthetic electron transport with a new type of multi-color PAM chlorophyll fluorometer.
784 Photosynthes Res 113, 127-144.
785 Seppälä, J., 2009. Fluorescence properties of Baltic Sea phytoplankton. Monograph of the Boreal
786 Environment Research 34, 80 pp.
787 Seppälä, J., Ylöstalo, P., Kaitala, S., Hällfors, S., Raateoja, M., Maunula, P., 2007. Ship-of-opportunity
788 based phycocyanin fluorescence monitoring of the filamentous cyanobacteria bloom dynamics in the
789 Baltic Sea. Estuar Coast Shelf Sci 73, 489-500.
790 Seppälä, J., Ylöstalo, P., Kuosa, H., 2005. Spectral absorption and fluorescence characteristics of
791 phytoplankton in different size fractions across a salinity gradient in the Baltic Sea. International Journal
792 of Remote Sensing 26, 387-414.
793 Silsbe, G., Oxborough, K., D.J., S., Forster, R., Ihnken, S., Komàrek, O., Lawrenz, E., Pràsil, O., Röttgers,
794 R., Sicner, M., Simis, S.G.H., Van Dijk, M.A., Kromkamp, J., 2015. Toward autonomous measurements
795 of photosynthetic electron transport rates: An evaluation of active fluorescence-based measurements of
796 photochemistry. Limnology & Oceanography: Methods 13, 138-155.
797 Simis, S.G.H., Huot, Y., Babin, M., Seppälä, J., Metsamaa, L., 2012. Optimization of variable
798 fluorescence measurements of phytoplankton communities with cyanobacteria. Photosynthes Res 112,
799 13-30.
800 Simis, S.G.H., Olsson, J., 2013. Unattended processing of shipborne hyperspectral reflectance
801 measurements. Remote Sensing of Environment 135, 202-212.
802 Stal, L.J., Albertano, P., Bergman, B., von Bröckel, K., Gallon, J.R., Hayes, P.K., Sivonen, K., Walsby,
803 A.E., 2003. BASIC: Baltic Sea cyanobacteria. An investigation of the structure and dynamics of water
804 blooms of cyanobacteria in the Baltic Sea - responses to a changing environment Cont Shelf Res 23,
805 1695-1714.
806 Steemann Nielsen, E., 1952. The Use of Radio-active Carbon (C^{14}) for Measuring Organic Production in
807 the Sea. ICES J Mar Sci 18, 117-140.
808 Suggett, D.J., MacIntyre, H.L., Geider, R.J., 2004. Evaluation of biophysical and optical determinations
809 of light absorption by photosystem II in phytoplankton. Limnol Oceanogr Methods 2, 316-332.
810 Suggett, D.J., Moore, C.M., Geider, J.R., 2010. Estimating Aquatic Productivity from Active
811 Fluorescence Measurements, in: Suggett, D.J. (Ed.), Chlorophyll *a* Fluorescence in Aquatic Sciences :
812 Methods and Applications. Springer Dordrecht Heidelberg, London, New York, pp 103-127.
813 Suggett, D.J., Moore, C.M., Hickman, A.E., Geider, R.J., 2009. Interpretation of fast repetition rate (FRR)
814 fluorescence: signatures of phytoplankton community structure versus physiological state. Mar Ecol Prog
815 Ser 376, 1-19.
816 Tamminen, T., Andersen, T., 2007. Seasonal phytoplankton nutirent limitation patterns as revealed by
817 bioassays over Baltic Sea gradients of salinity and eutrophication. Mar Ecol Prog Ser 340, 121-138.
818 Vassiliev, I.R., Prasil, O., Wyman, K.D., Kolber, Z., Hanson, A.K., Prentice, J.E., Falkowski, P., 1994.
819 Inhibition of PSII photochemistry by PAR and UV radiation in natural phytoplankton communities.
820 Photosynthes Res 42, 51-64.
821